Monotonically convergent algorithms for solving quantum optimal control problems of a dynamical system nonlinearly interacting with a control

Yukiyoshi Ohtsuki* and Kazuyuki Nakagami
Department of Chemistry, Graduate School of Science, Tohoku University, Sendai 980-8578, Japan and CREST, Japan Science and Technology Agency, 4-1-8 Honcho, Kawaguchi, Saitama 332-0012, Japan
(Received 19 December 2007; published 18 March 2008)

We develop a family of monotonically convergent iterative algorithms for solving a wide class of optimal control problems in which a dynamical system interacts *nonlinearly* with a control. The key idea is to divide a control into identical components and to introduce auxiliary steps to update each component at every iteration step. The algorithms are proved to exhibit monotonic convergence, which is also numerically confirmed through a case study of the control of molecular orientation. The numerical results show that high-quality solutions can be obtained by using the present algorithms.

DOI: 10.1103/PhysRevA.77.033414 PACS number(s): 33.80.Wz, 33.90.+h

I. INTRODUCTION

Quantum optimal control theory (OCT) provides a general and flexible tool of designing a control to best manipulate a dynamical system [1–3]. Control achievement is expressed as a quantitative criterion, called a cost functional. An optimal control is derived by maximizing or minimizing the cost functional, which leads to control design equations. As they are nonlinear coupled equations, it is often essential to develop efficient solution algorithms to perform OCT-based simulations. For this purpose, monotonically convergent algorithms [4–10] as well as the Krotov variants [11,12]) have been developed; however, these algorithms assume linear interactions with respect to a control.

There exist dynamical systems in which nonlinear interactions with a control play an important role. Examples include molecular dynamics in the presence of strong (nonresonant) laser fields [13], such as molecular alignment or orientation [14–19] and chemical reactions on distorted potential-energy surfaces [20,21]. In this regard, some attempts that apply optimal control simulations to such nonlinear problems have been reported, in which gradient methods [22–24], learning algorithms [25–27], an "approximately monotonic" convergent algorithm [28], and so on [29] are adopted.

The purpose of the present work is to develop a family of monotonically convergent algorithms to solve optimal control problems of a dynamical system that nonlinearly interacts with a control. Coupled equations are derived from the two basic cost functionals, which are referred to as type I and type II, that can describe a wide range of applications for designing controls. The present algorithms are proved to exhibit monotonic convergence. The algorithmic performance is numerically illustrated through a case study of the control of molecular orientation. In Sec. II, control design equations are derived. We present the algorithms in the case of a second-order interaction (Sec. III) and in the general case of an Nth-order interaction (Sec. IV). The algorithms for solving penalty-free optimal control problems are presented in Sec. V. Some exceptional cases are discussed in Sec. VI. In Sec. VII, numerical tests are implemented in a rigid-rotor model system.

*Author to whom correspondence should be addressed: y-ohtsuki@mail.tains.tohoku.ac.jp

II. CONTROL DESIGN EQUATIONS

The system concerned here is assumed to be specified by a state vector $|u(t)\rangle$, which can be a wave function, a quantum density operator, and so on. The system interacts with a time-dependent control, $E(t)$, linearly through operator β_1 and nonlinearly through $\beta_n (n=2,3,\ldots,N)$. The equation of motion is expressed as

$$\frac{\partial}{\partial t}|u(t)\rangle = \sum_{n=0}^{N} \beta_n [E(t)]^n |u(t)\rangle, \tag{1}$$

where β_0 represents the field-free operator. All operators β_n $(n=0,1,\ldots,N)$, which can be non-Hermitian, do not depend on the control.

An optimal pulse maximizes or minimizes the cost functional that quantitatively expresses a control objective. Here we introduce two basic functionals F_I and F_{II} to quantitatively evaluate control achievement [6,9,10,30]:

$$F_I = 2\,\mathrm{Re}\langle X|u(t_f)\rangle + 2\,\mathrm{Re}\int_0^{t_f} dt \langle Y(t)|u(t)\rangle \tag{2}$$

and

$$F_{II} = \langle u(t_f)|X|u(t_f)\rangle + \int_0^{t_f} dt \langle u(t)|Y(t)|u(t)\rangle. \tag{3}$$

The type-I (type-II) functional has a linear (bilinear) form with respect to the state vector. In Eq. (2), a target state at a final time is specified by vector $|X\rangle$, while an intermediate target over the control period is specified by $|Y(t)\rangle$. In the case of the type-II functional, the physical targets are specified by two non-negative, semidefinite Hermitian operators X and $Y(t)$. The optimal pulse is often designed subject to a minimum penalty, which is defined by

$$G = \int_0^{t_f} dt \frac{1}{\lambda(t)} [E(t)]^2. \quad (4)$$

Here a positive function $\lambda(t)$ weighs the physical significance of the penalty.

Taking into account the penalty, gross control achievement is assessed by $J_I = F_I - G$ and $J_{II} = F_{II} - G$. The coupled pulse design equations are derived by applying the calculus of variations to these basic functionals J_I and J_{II}. In both cases, the optimal pulse is expressed as

$$E(t) = \lambda(t) \sum_{n=1}^{N} \mathrm{Re}\langle \xi(t)| n\beta_n [E(t)]^{n-1} |u(t)\rangle, \quad (5)$$

where $|\xi(t)\rangle$ is the Lagrange multiplier that represents the constraint of satisfying the equation of motion, Eq. (1). In the type-I case, the equation of motion for the Lagrange multiplier is given by

$$\frac{\partial}{\partial t}|\xi(t)\rangle = -\sum_{n=0}^{N} \beta_n^\dagger [E(t)]^n |\xi(t)\rangle - |Y(t)\rangle, \quad (6)$$

with a final condition $|\xi(t_f)\rangle = |X\rangle$. In the type-II case, the Lagrange multiplier obeys the equation

$$\frac{\partial}{\partial t}|\xi(t)\rangle = -\sum_{n=0}^{N} \beta_n^\dagger [E(t)]^n |\xi(t)\rangle - Y(t)|u(t)\rangle, \quad (7)$$

with a final condition $|\xi(t_f)\rangle = X|u(t_f)\rangle$. Equations (1), (5), and (6) [Eqs. (1), (5), and (7)] compose the coupled-control design equations in the type-I [type-II] case.

In the subsequent sections, we develop monotonically convergent algorithms for iteratively solving the control design equations. The key idea is to divide the control $E(t)$ into N identical components $\{E_n(t);\ n=1,2,\ldots,N\}$. All the expressions associated with the control in the control design equations are represented by the symmetrical sum of products of these identical components. In each iteration step, N auxiliary steps are introduced, in which one of the components is updated. After the convergence, all the divided components should be identical to each other.

III. SOLUTION ALGORITHM AND ITS CONVERGENCE BEHAVIOR IN THE TYPE-I (N=2) CASE

For the sake of providing concrete descriptions, we first consider the type-I case with $N=2$. When the solution algorithm starts the iteration with $|u_n^{(0)}(t)\rangle$ using an appropriate initial trial control $E_n^{(0)}(t)$ $(n=1,2)$, the control design equations at the kth iteration step $(k \geq 1)$ are summarized as follows.

Auxiliary step 1:

$$\frac{\partial}{\partial t}|\xi_1^{(k)}(t)\rangle = -\left\{ \beta_0^\dagger + \frac{\beta_1^\dagger}{2}[\bar{E}_1^{(k)}(t) + E_2^{(k-1)}(t)] + \beta_2^\dagger \bar{E}_1^{(k)}(t) E_2^{(k-1)}(t) \right\} |\xi_1^{(k)}(t)\rangle - |Y(t)\rangle \quad (8)$$

and

$$\frac{\partial}{\partial t}|u_1^{(k)}(t)\rangle = -\left\{ \beta_0 + \frac{\beta_1}{2}[E_1^{(k)}(t) + E_2^{(k-1)}(t)] + \beta_2 E_1^{(k)}(t) E_2^{(k-1)}(t) \right\} |u_1^{(k)}(t)\rangle, \quad (9)$$

where the controls are expressed as

$$\bar{E}_1^{(k)}(t) = \lambda(t) \mathrm{Re}\langle \xi_1^{(k)}(t)| [\beta_1 + 2\beta_2 E_2^{(k-1)}(t)] |u_2^{(k-1)}(t)\rangle \quad (10)$$

and

$$E_1^{(k)}(t) = \lambda(t) \mathrm{Re}\langle \xi_1^{(k)}(t)| [\beta_1 + 2\beta_2 E_2^{(k-1)}(t)] |u_1^{(k)}(t)\rangle. \quad (11)$$

Auxiliary step 2:

$$\frac{\partial}{\partial t}|\xi_2^{(k)}(t)\rangle = -\left\{ \beta_0^\dagger + \frac{\beta_1^\dagger}{2}[E_1^{(k)}(t) + \bar{E}_2^{(k)}(t)] + \beta_2^\dagger E_1^{(k)}(t) \bar{E}_2^{(k)}(t) \right\} \times |\xi_2^{(k)}(t)\rangle - |Y(t)\rangle \quad (12)$$

and

$$\frac{\partial}{\partial t}|u_2^{(k)}(t)\rangle = -\left\{ \beta_0 + \frac{\beta_1}{2}[E_1^{(k)}(t) + E_2^{(k)}(t)] + \beta_2 E_1^{(k)}(t) E_2^{(k)}(t) \right\} \times |u_2^{(k)}(t)\rangle, \quad (13)$$

where the controls are expressed as

$$\bar{E}_2^{(k)}(t) = \lambda(t) \mathrm{Re}\langle \xi_2^{(k)}(t)| [\beta_1 + 2\beta_2 E_1^{(k)}(t)] |u_1^{(k)}(t)\rangle \quad (14)$$

and

$$E_2^{(k)}(t) = \lambda(t) \mathrm{Re}\langle \xi_2^{(k)}(t)| [\beta_1 + 2\beta_2 E_1^{(k)}(t)] |u_2^{(k)}(t)\rangle. \quad (15)$$

The final and initial conditions are given by $|\xi_n^{(k)}(t_f)\rangle = |X\rangle$ and $|u_n^{(k)}(0)\rangle = |u_0\rangle$ $(n=1,2)$, respectively.

To prove the monotonic convergence behavior, we consider the difference in cost functionals between the kth and $(k-1)$th adjacent iteration steps:

$$\delta J_I^{(k,k-1)} = J_I^{(k)} - J_I^{(k-1)} = \delta F_I^{(k,k-1)} - \delta G^{(k,k-1)}. \quad (16)$$

Here we introduce the control achievement after the first auxiliary step, which is defined by

$$F_I^{(k-1/2)} = 2\ \mathrm{Re}\langle X|u_1^{(k)}(t_f)\rangle + 2\ \mathrm{Re}\int_0^{t_f} dt \langle Y(t)|u_1^{(k)}(t)\rangle. \quad (17)$$

Then, we have

$$\delta F_I^{(k,k-1)} = [F_I^{(k)} - F_I^{(k-1/2)}] + [F_I^{(k-1/2)} - F_I^{(k-1)}] \equiv \delta F_2 + \delta F_1, \quad (18)$$

where δF_n $(n=1,2)$ is written as

$$\delta F_n = 2\ \mathrm{Re}\langle X|\delta u_n^{(k)}(t_f)\rangle + 2\ \mathrm{Re}\int_0^{t_f} dt \langle Y(t)|\delta u_n^{(k)}(t)\rangle, \quad (19)$$

with $|\delta u_n^{(k)}(t)\rangle = |u_n^{(k)}(t)\rangle - |u_{n-1}^{(k)}(t)\rangle$ $(|u_0^{(k)}(t)\rangle \equiv |u_2^{(k-1)}(t)\rangle)$. It is convenient to introduce a function

$$P_n^{(k)}(t) = 2\,\mathrm{Re}\langle \xi_n^{(k)}(t)|\delta u_n^{(k)}(t)\rangle, \tag{20}$$

which gives $P_n^{(k)}(t_f)=2\,\mathrm{Re}\langle X|\,\delta u_n^{(k)}(t_f)\rangle$ and $P_n^{(k)}(0)=0$. In the case of $n=2$, for example, by differentiating Eq. (20) with respect to time, we obtain

$$\begin{aligned}\frac{d}{dt}P_2^{(k)}(t) &= [E_2^{(k)}(t)-\bar{E}_2^{(k)}(t)]\mathrm{Re}\langle \xi_2^{(k)}(t)|[\beta_1+2\beta_2E_1^{(k)}(t)]\\ &\quad\times|u_2^{(k)}(t)\rangle + [\bar{E}_2^{(k)}(t)-E_2^{(k-1)}(t)]\mathrm{Re}\langle \xi_2^{(k)}(t)|\\ &\quad\times[\beta_1+2\beta_2E_1^{(k)}(t)]|u_1^{(k)}(t)\rangle - 2\,\mathrm{Re}\langle Y(t)|\delta u_2^{(k)}(t)\rangle.\end{aligned} \tag{21}$$

Substituting Eqs. (14) and (15) into Eq. (21) and then integrating the resulting equation over $[0,t_f]$, we have

$$\begin{aligned}\delta F_2 = \int_0^{t_f}\frac{dt}{2\lambda(t)}\{&[E_2^{(k)}(t)-\bar{E}_2^{(k)}(t)]E_2^{(k)}(t)\\ &+[\bar{E}_2^{(k)}(t)-E_2^{(k-1)}(t)]\bar{E}_2^{(k)}(t)\}.\end{aligned} \tag{22}$$

Similarly, we derive

$$\begin{aligned}\delta F_1 = \int_0^{t_f}\frac{dt}{2\lambda(t)}\{&[E_1^{(k)}(t)-\bar{E}_1^{(k)}(t)]E_1^{(k)}(t)\\ &+[\bar{E}_1^{(k)}(t)-E_1^{(k-1)}(t)]\bar{E}_1^{(k)}(t)\}.\end{aligned} \tag{23}$$

As the penalty term at the kth step is expressed as

$$G^{(k)} = \int_0^{t_f}\frac{dt}{2\lambda(t)}\{[E_1^{(k)}(t)]^2+[E_2^{(k)}(t)]^2\}, \tag{24}$$

in the present algorithm, the substitution of Eqs. (22)–(24) into Eq. (16) yields

$$\begin{aligned}\delta J_I^{(k,k-1)} &= \int_0^{t_f}\frac{dt}{2\lambda(t)}\{[E_2^{(k)}(t)-\bar{E}_2^{(k)}(t)]^2+[\bar{E}_2^{(k)}(t)-E_2^{(k-1)}(t)]^2\\ &\quad+[E_1^{(k)}(t)-\bar{E}_1^{(k)}(t)]^2+[\bar{E}_1^{(k)}(t)-E_1^{(k-1)}(t)]^2\}\\ &\geq 0,\end{aligned} \tag{25}$$

which proves the monotonic convergence behavior. In the present algorithm, the control is artificially divided into two identical components $E_1(t)$ and $E_2(t)$. We show that the two components actually approach the same control. Let $E_n(t)$ be the limit of $E_n^{(k)}(t)$ as $k\to\infty$. Because of the symmetric form of the interaction terms with respect to the auxiliary step numbers $\{n\}$, the state vectors approach n-independent states—i.e., $|u_n^{(k)}(t)\rangle\to|u(t)\rangle$ and $|\xi_n^{(k)}(t)\rangle\to|\xi(t)\rangle$ as $k\to\infty$. From Eqs. (11) and (15), we have

$$E_1(t) = \lambda(t)\mathrm{Re}\langle \xi(t)|[\beta_1+2\beta_2E_2(t)]|u(t)\rangle \tag{26}$$

and

$$E_2(t) = \lambda(t)\mathrm{Re}\langle \xi(t)|[\beta_1+2\beta_2E_1(t)]|u(t)\rangle, \tag{27}$$

which lead to $E_1(t)=E_2(t)$.

Taking advantage of the flexibility of the algorithm, we can simplify the iteration procedure. For example, each iteration step can be described without using $\bar{E}_n^k(t)$ $(n=1,2)$ as

$$\begin{aligned}\frac{\partial}{\partial t}|\xi^{(k)}(t)\rangle = -\Bigg\{&\beta_0^\dagger+\frac{\beta_1^\dagger}{2}[E_1^{(k)}(t)+E_2^{(k-1)}(t)]\\ &+\beta_2^\dagger E_1^{(k)}(t)E_2^{(k-1)}(t)\Bigg\}|\xi^{(k)}(t)\rangle - |Y(t)\rangle,\end{aligned} \tag{28}$$

with the final condition $|\xi^{(k)}(t_f)\rangle=|X\rangle$, and

$$\begin{aligned}\frac{\partial}{\partial t}|u^{(k)}(t)\rangle = -\left\{\beta_0+\frac{\beta_1}{2}[E_1^{(k)}(t)+E_2^{(k)}(t)]+\beta_2E_1^{(k)}(t)E_2^{(k)}(t)\right\}\\ \times|u^{(k)}(t)\rangle,\end{aligned} \tag{29}$$

with the initial condition $|u^{(k)}(0)\rangle=|u_0\rangle$. The controls at the kth step are expressed as

$$E_1^{(k)}(t) = \lambda(t)\mathrm{Re}\langle \xi^{(k)}(t)|[\beta_1+2\beta_2E_2^{(k-1)}(t)]|u^{(k-1)}(t)\rangle \tag{30}$$

and

$$E_2^{(k)}(t) = \lambda(t)\mathrm{Re}\langle \xi^{(k)}(t)|[\beta_1+2\beta_2E_1^{(k)}(t)]|u^{(k)}(t)\rangle. \tag{31}$$

IV. SOLUTION ALGORITHM IN A GENERAL CASE

We extend the algorithm developed in the previous section to a general case in which the equation of motion of the system is given by Eq. (1). The symmetrically divided component that is improved at the nth auxiliary step of the kth iteration step is written as $E_n^{(k)}(t)$ $(1\leq n\leq N)$. We also introduce $\bar{E}_n^{(k)}(t)$ that connects the nth auxiliary step with the previous auxiliary step. It is convenient to introduce the following notation to systematically represent the algorithms:

$$\bar{\epsilon}_{(n)j}^{(k)}(t) = \begin{cases} E_j^{(k)}(t) & (j<n),\\ \bar{E}_n^{(k)}(t) & (j=n),\\ E_j^{(k-1)}(t) & (j>n),\end{cases} \tag{32}$$

and

$$\epsilon_{(n)j}^{(k)}(t) = \begin{cases} E_j^{(k)}(t) & (j\leq n),\\ E_j^{(k-1)}(t) & (j>n).\end{cases} \tag{33}$$

The components $\bar{E}_n^{(k)}(t)$ and $E_n^{(k)}(t)$ are, respectively, expressed as

$$\bar{E}_n^{(k)}(t) = \lambda(t)\mathrm{Re}\langle \xi_n^{(k)}(t)|B_n^{(k)}|u_{n-1}^{(k)}(t)\rangle \tag{34}$$

and

$$E_n^{(k)}(t) = \lambda(t)\mathrm{Re}\langle \xi_n^{(k)}(t)|B_n^{(k)}|u_n^{(k)}(t)\rangle, \tag{35}$$

where $|u_0^{(k)}(t)\rangle \equiv |u_N^{(k-1)}(t)\rangle$. In Eqs. (34) and (35), the operator $B_n^{(k)}$ is defined by

$$B_n^{(k)} = \beta_1 + \sum_{m=2}^{N} \frac{N\beta_m}{{}_N C_m} \sum_{j_1<\cdots<j_{m-1}}^{N}{}^{(n)} \epsilon_{(n)j_1}^{(k)}(t) \cdots \epsilon_{(n)j_{m-1}}^{(k)}(t), \tag{36}$$

where

$$\sum_{j_1<\cdots<j_{m-1}}^{N}{}^{(n)} \equiv \sum_{j_1<\cdots<j_{m-1}}^{N} (j_1 \neq n, \ldots, j_{m-1} \neq n). \tag{37}$$

We consider the solution algorithm that starts the iteration with $|u_N^{(0)}\rangle$ using an appropriate initial trial control $E_n^{(0)}(n=1,2,\ldots,N)$. The type-I control design equations at the nth auxiliary step of the kth iteration step $(k\geq 1)$ are

$$\frac{\partial}{\partial t}|\xi_n^{(k)}(t)\rangle = -\left\{ \beta_0^{\dagger} + \sum_{m=1}^{N} \frac{\beta_m^{\dagger}}{{}_N C_m} \sum_{j_1<\cdots<j_m}^{N} \bar{\epsilon}_{(n)j_1}^{(k)}(t) \cdots \bar{\epsilon}_{(n)j_m}^{(k)}(t) \right\} \times |\xi_n^{(k)}(t)\rangle - |Y(t)\rangle, \tag{38}$$

with the final condition $|\xi_n^{(k)}(t_f)\rangle = |X\rangle$, and

$$\frac{\partial}{\partial t}|u_n^{(k)}(t)\rangle = \left\{ \beta_0 + \sum_{m=1}^{N} \frac{\beta_m}{{}_N C_m} \sum_{j_1<\cdots<j_m}^{N} \epsilon_{(n)j_1}^{(k)}(t) \cdots \epsilon_{(n)j_m}^{(k)}(t) \right\} \times |u_n^{(k)}(t)\rangle, \tag{39}$$

with the initial condition $|u_n^{(k)}(0)\rangle = |u_0\rangle$. In the case of the type-II control, instead of Eq. (38), the equation of motion for the Lagrange multiplier is expressed as

$$\frac{\partial}{\partial t}|\xi_n^{(k)}(t)\rangle = -\left\{ \beta_0^{\dagger} + \sum_{m=1}^{N} \frac{\beta_m^{\dagger}}{{}_N C_m} \sum_{j_1<\cdots<j_m}^{N} \bar{\epsilon}_{(n)j_1}^{(k)}(t) \cdots \bar{\epsilon}_{(n)j_m}^{(k)}(t) \right\} \times |\xi_n^{(k)}(t)\rangle - Y(t)|u_{n-1}^{(k)}(t)\rangle, \tag{40}$$

where the final condition is given by $|\xi_n^{(k)}(t_f)\rangle = X|u_{n-1}^{(k)}(t_f)\rangle$.

For the type-I control, the monotonic convergence behavior is proved in the Appendix. Similarly, we can prove the monotonic convergence behavior in the type-II case (not shown), provided that the Hermitian target operators X and $Y(t)$ are non-negative and semidefinite. Note that we can introduce an inhomogeneous term and/or a dissipation term into the equation of motion (1) without changing the above algorithms. The present algorithms also allow the dynamical system to be a classical one, as long as the equations of motion have a linear form in the system state.

V. ALGORITHMS FOR SOLVING PENALTY-FREE OPTIMAL CONTROL PROBLEMS

Similar algorithms to those developed in the previous sections are applicable to optimal control problems that do not include the penalty term, Eq. (4). Cost functionals in type-I and type-II cases are given by $J_I = F_I$ and $J_{II} = F_{II}$, respectively. Considering the nth auxiliary step of the kth iteration step in the type-I case, we have the same equations as Eqs. (38) and (39), in which the controls now should be replaced with the following expressions:

$$\bar{E}_n^{(k)}(t) = \bar{E}_n^{(k-1)}(t) + \delta\bar{\epsilon}_n^{(k)}(t) \tag{41}$$

and

$$E_n^{(k)}(t) = E_n^{(k-1)}(t) + \delta\epsilon_n^{(k)}(t), \tag{42}$$

with

$$\delta\bar{\epsilon}_n^{(k)}(t) = \lambda_n^{(k)}(t)\mathrm{Re}\langle \xi_n^{(k)}(t)|B_n^{(k)}|u_{n-1}^{(k)}(t)\rangle \tag{43}$$

and

$$\delta\epsilon_n^{(k)}(t) = \lambda_n^{(k)}(t)\mathrm{Re}\langle \xi_n^{(k)}(t)|B_n^{(k)}|u_n^{(k)}(t)\rangle. \tag{44}$$

As the exclusion of a penalty removes a portion of the constraints from the optimal control problems, some degree of flexibility is introduced into the above solution algorithm. In fact, the positive function $\lambda_n^{(k)}(t)$ is a convergence parameter rather than the amplitude function that weighs the physical significance of the penalty. It can have a step-dependent value that characterizes the convergence behavior of the algorithm.

The monotonic convergence behavior of the algorithm is proved in the same way as that described in Sec. IV. Following the Appendix, the difference in type-I cost functionals between kth and $(k-1)$th adjacent iteration steps is given by

$$\delta J_I^{(k,k-1)} = \sum_{n=1}^{N} \int_0^{t_f} \frac{dt}{N\lambda_n^{(k)}(t)} \{[\delta\epsilon_n^{(k)}(t)]^2 + [\delta\epsilon_n^{(k)}(t) - \delta\bar{\epsilon}_n^{(k)}(t)]^2 + [\delta\bar{\epsilon}_n^{(k)}(t)]^2\} \geq 0, \tag{45}$$

which proves the monotonic convergence. If the iterative calculation converges, we have $\delta\bar{\epsilon}_n^{(k)}(t) = \delta\epsilon_n^{(k)}(t) = 0$, which leads to

$$\mathrm{Re}\langle \xi_n^{(k)}(t)|B_n^{(k)}|u_n^{(k)}(t)\rangle = 0. \tag{46}$$

This gives the first-order variational optimality condition $\delta J_I = 0$.

We have a similar monotonic convergence algorithm for the type-II functional (not shown). As shown in Secs. III and IV, we can even skip some of the auxiliary steps needed to calculate $\delta\bar{\epsilon}_n^{(k)}(t)$, while retaining the monotonic convergence behavior of the algorithms.

VI. EXCEPTIONAL CASES

There are cases in which the algorithms in Secs. III and IV cannot be used. As an example, consider the type-I cost functional that contains the penalty. In the present work, the penalty is expressed as the integral of the square of the control over the control period, $t\in[0,t_f]$. If there is only a second-order interaction with respect to a control in the equation of motion, then the expression of the optimal control in Eq. (5) is reduced to

$$2\lambda(t)\mathrm{Re}\langle\xi(t)|\beta_2|u(t)\rangle = 1. \tag{47}$$

As the control does not appear explicitly in Eq. (47), the algorithms developed in Sec. III cannot be used to solve the control design equations. One idea would be to add an artificial linear interaction term with a negligibly small value. However, we have checked that such a procedure introduced numerical instabilities and no optimal solution can be obtained.

Here we briefly comment on how to overcome this difficulty. One approach is to adopt a penalty-free cost functional that does not contain the penalty. An alternative approach [31] is to add an appropriate reference control $E_{ref}(t)$ to the control to be designed in order to introduce a time-dependent linear interaction term in Eq. (47). Through numerical tests (not shown), we have confirmed that these two approaches provide an effective means to obtain stable solutions. A third approach is to modify the penalty term in which, for example, the integrand is expressed as a quartic form with respect to a control. In this case, the equation of motion has a linear interaction with respect to $I(t)=[E(t)]^2$ and the integrand in the penalty has a quadratic form with respect to $I(t)$. Then, a conventional monotonically convergent algorithm is used to solve the coupled design equations expressed in terms of $I(t)$. However, we have seen that this procedure often leads to a negative solution (not shown), which is inconsistent with the non-negative property of $I(t)$.

VII. NUMERICAL TESTS

Numerical tests are implemented in the orientation control of a rigid rotor that models the rotational states of HCN in its electronic ground state [28]. In the present examples, we consider the case where penalty costs are taken into account. The primary purpose here is to numerically evaluate the convergence behavior of the algorithms rather than to examine control mechanisms.

We assume that the system interacts with a linearly polarized time-dependent electric field $E(t)$ coupled through a permanent dipole moment μ and polarizability components $\alpha_\parallel$ and $\alpha_\perp$. Then, the Hamiltonian is expressed as

$$H^t = B\hat{J}^2 - \mu E(t)\cos\,\theta - [(\alpha_\parallel - \alpha_\perp)\cos^2\,\theta + \alpha_\perp]\frac{E^2(t)}{2}, \tag{48}$$

where B is the rotational constant, $\hat{J}$ is the angular momentum operator, and θ is the polar angle between the polarization vector of the laser and the molecular axis. As we are concerned with the orientation control by resonant rotational excitation processes [25,28,29], both the permanent dipole and polarizability coupling terms are included in Eq. (48). (Note that if we use a laser with higher frequencies that induces nonresonant excitation processes, the Hamiltonian can be replacaed by a time-averaged one that solely contains the induced interaction with a pulse envelope [32,33].) The time evolution of the system is described by a density operator $\rho(t)$ that obeys the quantum Liouville equation

$$i\hbar\frac{\partial}{\partial t}\rho(t) = [H^t, \rho(t)]. \tag{49}$$

In the following simulations, time and energy are measured in units of the rotational period, $T_{rot}=h/2B$ and $\hbar/T_{rot}$, respectively, whereby the electric field is expressed as $\mu E(t)/B$. The density operator is expanded in terms of spherical harmonics $Y_{J,M}$, and the time evolution of the expansion coefficients is numerically integrated by the Runge-Kutta-Fehlberg method.

Our aim here is to achieve the orientation control at a specified final time. In the following, we assume $t_f=15$ in units of T_{rot} as an example. The relation between the choice of a final time and control mechanisms will be discussed elsewhere. The control achievement is evaluated by the type-I ($N=2$) functional with a penalty term, in which the target vectors are set to $X=(\cos\,\theta)/2$ and $Y(t)=0$. To assure smooth rise and decay of a control pulse, we introduce the amplitude function in the penalty that is expressed as

$$\lambda(t) = \begin{cases} \lambda_0 \sin(\pi t/2\Delta) & (0 < t < \Delta), \\ \lambda_0 & (\Delta < t < t_f - \Delta), \\ \lambda_0 \sin[\pi(t_f - t/2\Delta)] & (t_f - \Delta < t < t_f), \end{cases} \tag{50}$$

with $\Delta=2$. The coupled pulse design equations are solved by using the simplified iteration algorithm shown in the last paragraph of Sec. III. As we are concerned with the performance of the solution algorithm, we consider the zero-temperature case below, in which the lowest 11 basis functions are sufficient for computational purposes. When we adopted the original value of the polarizability, we could not find any effects originating from the induced dipole in our numerical examples. Because our purpose here is to evaluate the algorithmic performance in the presence of a nonlinear interaction, in the following simulations, we assume a fictitious model system that has 10^4 (Figs. 1 and 2) and 10^5 (Figs. 3 and 4) times larger values for the polarizability components.

Figure 1 shows the convergence behavior for $\lambda_0=1$, 3, and 10. When the difference in value of the adjacent functionals is smaller than 10^{-7}, we regard the calculation as converged. The converged value of the cost functional is denoted by J. In Fig. 1, the ordinate shows the logarithm of the difference between J and the cost functional at the kth iteration step $J^{(k)}$. The abscissa represents the logarithm of the number of iteration steps, k. We observe monotonic convergence although the number of iteration steps required to achieve the convergence considerably depends on the value of λ_0. The larger value of λ_0 leads to better control achievement, which may result in greater difficulty in finding the optimal solution. We also see small oscillating structures. This could be because we used the simplified algorithms in which some of the auxiliary steps are neglected and/or because of the intrinsic numerical difficulty in the solution search originating from the interaction via the polarizability.

Figure 2(a) shows the optimal pulse in the case of $\lambda_0=10$ (solid line) and the initial trial pulse (dotted line). In our scheme, we artificially divide the electric field into two components in a symmetrical fashion. As these components con-

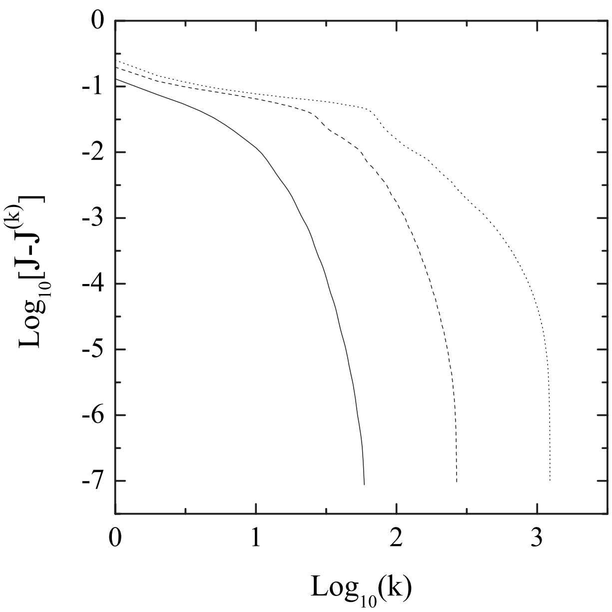

FIG. 1. Convergence behavior when $\lambda_0=1$ (solid line), $\lambda_0=3$ (dashed line), and $\lambda_0=10$ (dotted line).

verge virtually to a single limit, we cannot recognize the difference in Fig. 1(a). The time evolution of the target expectation value is plotted in Fig. 2(b). At the final time, it has a value of 90.0%.

To more clearly see the effects of the polarizability on the convergence behavior, here we assume 10^5 times larger values for the polarizability components. In this example, we set the amplitude parameter and the convergence criterion to $\lambda_0=10$ and 10^{-9}, respectively. Starting with the initial trial field shown in Fig. 1(a), the calculation converges after 360 iteration steps. Figure 3(a) shows the difference between symmetrically divided electric field components, $E_1(t)-E_2(t)$. Unlike the results in Fig. 1(a), we can see a non-negligible difference between $E_1(t)$ and $E_2(t)$. We calculated

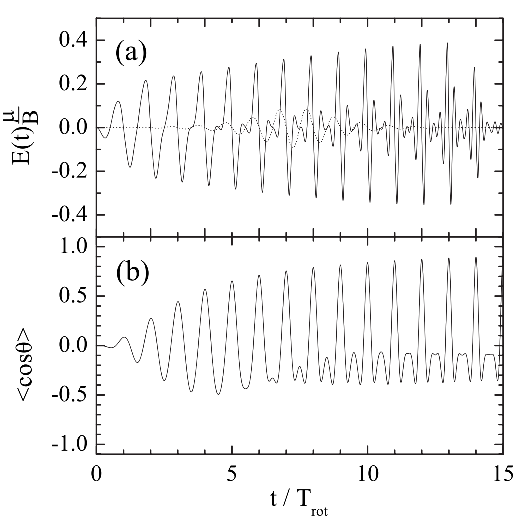

FIG. 2. (a) Optimal pulse in the case of $\lambda_0=10$ (solid line) and initial trial pulse (dotted line). Time is measured in units of the rotational period, $T_{rot}=h/2B$ (also see text). (b) Target expectation value as a function of time.

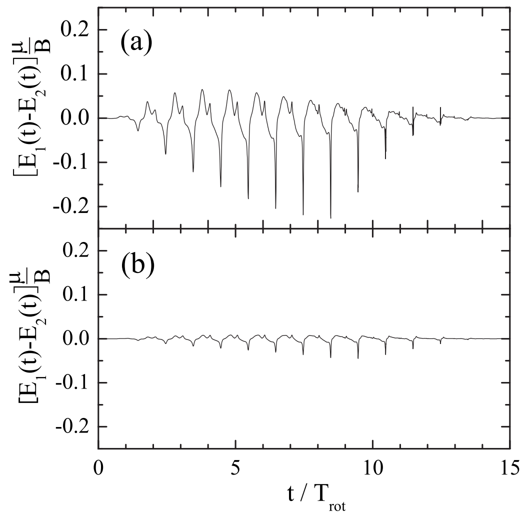

FIG. 3. (a) Difference between symmetrically divided electric field components, $E_1(t)-E_2(t)$. (b) Difference $E_1(t)-E_2(t)$ after two extra calculations (see text).

the target expectation values by using $E(t)=\eta E_1(t)+(1-\eta)E_2(t)$ for several values of $\eta\in[0,1]$ and found that the expectation values hardly depended on the choice of $E(t)$. Polarizability couples with the square of an electric field, which introduces ambiguity in the phase of the electric field. This could reduce the sensitivity in searching for an optimal solution. To reduce the difference, for example, we can restart the iteration with the averaged electric field $[E_1(t)+E_2(t)]/2$. As shown in Fig. 3(b), the difference becomes much smaller than that in Fig. 3(a). The result in Fig. 3(b) is obtained by performing such extra calculations two times. In the first (second) extra calculation, 169 (7) iteration steps are required to meet the convergence criterion.

Figure 4(a) shows the optimal pulse after the two extra calculations. The pulse is characterized by a highly asym--metric structure. Such an asymmetry introduces asymmetric interaction into the molecule, which leads to efficient orien-

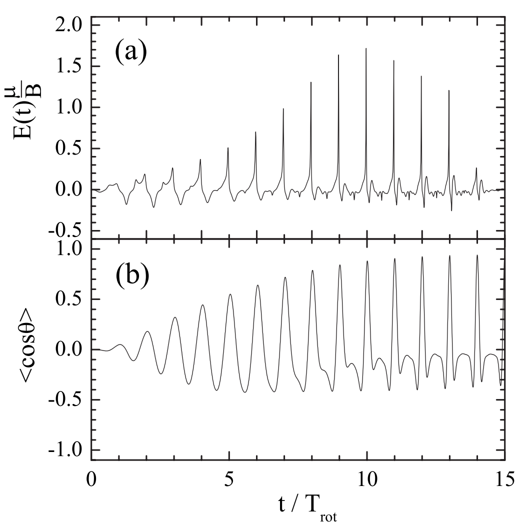

FIG. 4. (a) Optimal pulse after two extra calculations [Fig. 3(b)]. (b) Target expectation value as a function of time.

tation control. From Fig. 4(b), the time-dependent expectation value has a value of 94.2% at the final time.

VIII. SUMMARY

We have presented a family of monotonically convergent algorithms to solve quantum optimal control problems, in which a system interacts nonlinearly with a control. Control design equations are derived from two basic functionals—i.e., type-I and type-II functionals—which describe a wide range of physical criteria with or without being subjected to control costs. We presented algorithms when the equation of motion includes nonlinear interaction up to the second order in a control (Sec. III), those in a general case, in which the equation of motion includes nonlinear interactions up to an arbitrary order (Sec. IV), and those for solving penalty-free optimal control problems (Sec. V). We have proved that all the algorithms exhibit monotonic convergence. In Sec. VI, we examined exceptional situations in which the local optimality condition does not lead to the expression of a control in an explicit form and discussed several practical ways to overcome the difficulty. In Sec. VII, to numerically show the algorithmic performance through a case study, we have applied the algorithms to the orientation control of a rigid rotor that models the rotational dynamics of HCN in the electronic ground state. In the examples, the penalty costs are taken into account. A high degree of orientation is achieved by controlled rotational transitions through electric dipole and polarizability interactions. Numerical results confirm that the present algorithms show monotonic convergence behavior and possess high sensitivity in searching for optimal solutions.

When a dynamical system linearly interacts with a control, optimal control simulations are typically done by using monotonically convergent algorithms. As the present algorithms possess monotonically convergent properties, they can be useful tools for solving optimal control problems of a dynamical system nonlinearly interacting with a control.

ACKNOWLEDGMENT

This work was supported in part by a Grant-in-Aid for scientific research on priority areas, "Molecular theory for real systems" (Area No. 461), from the Ministry of Education, Culture, Sports, Science and Technology, Japan.

APPENDIX: PROOF OF THE MONOTONIC CONVERGENCE OF TYPE-I ALGORITHMS

Consider the difference in cost functional between the kth and $(k-1)$th adjacent iteration steps:

$$\delta J_I^{(k,k-1)} = J_I^{(k)} - J_I^{(k-1)} = \delta F_I^{(k,k-1)} - \delta G^{(k,k-1)}, \tag{A1}$$

where the difference in penalty term is expressed as

$$\delta G^{(k,k-1)} = \int_0^{t_f} \frac{dt}{N\lambda(t)} \sum_{n=1}^{N} \{[E_n^{(k)}(t)]^2 - [E_n^{(k-1)}(t)]^2\}. \tag{A2}$$

We introduce an auxiliary functional that evaluates control achievement at the nth auxiliary step of the kth iteration step:

$$F_I^{(k-1+n/N)} = 2\,\mathrm{Re}\langle X|u_n^{(k)}(t_f)\rangle + 2\,\mathrm{Re}\int_0^{t_f} dt \langle Y(t)|u_n^{(k)}(t)\rangle, \tag{A3}$$

with $n=1,2,\ldots,N-1$. Using the auxiliary functional, the difference $\delta F_I^{(k,k-1)}$ is expressed as

$$\delta F_I^{(k,k-1)} = \sum_{n=1}^{N} [F_I^{(k-1+n/N)} - F_I^{[k-1+(n-1)/N]}] \equiv \sum_{n=1}^{N} \delta F_n. \tag{A4}$$

Substituting Eq. (A3) into δF_n, we have

$$\delta F_n = 2\,\mathrm{Re}\langle X|\delta u_n^{(k)}(t_f)\rangle + 2\,\mathrm{Re}\int_0^{t_f} dt \langle Y(t)|\delta u_n^{(k)}(t)\rangle, \tag{A5}$$

where $|\delta u_n^{(k)}(t)\rangle = |u_n^{(k)}(t)\rangle - |u_{n-1}^{(k)}(t)\rangle$ with $|u_0^{(k)}(t)\rangle = |u_N^{(k-1)}(t)\rangle$.

To express δF_n in terms of controls, we introduce a function

$$P_n^{(k)}(t) = 2\,\mathrm{Re}\langle \xi_n^{(k)}(t)|\delta u_n^{(k)}(t)\rangle, \tag{A6}$$

whose initial and final values are given by $P_n^{(k)}(0)=0$ and $P_n^{(k)}(t_f) = 2\,\mathrm{Re}\langle X|\delta u_n^{(k)}(t_f)\rangle$, respectively.

Differentiating Eq. (A6) with respect to time, we have

$$\begin{aligned}\frac{d}{dt}P_n^{(k)}(t) + 2\,\mathrm{Re}\langle Y(t)|\delta u_n^{(k)}(t)\rangle ={}& -2\,\mathrm{Re}\langle \xi_n^{(k)}(t)|\sum_{m=1}^{N} \frac{\beta_m}{{}_N C_m} \sum_{j_1<\cdots<j_m}^{N} \bar{\epsilon}_{(n)j_1}^{(k)}(t)\cdots \bar{\epsilon}_{(n)j_m}^{(k)}(t)|\delta u_n^{(k)}(t)\rangle \\ &+ 2\,\mathrm{Re}\langle \xi_n^{(k)}(t)|\sum_{m=1}^{N} \frac{\beta_m}{{}_N C_m} \sum_{j_1<\cdots<j_m}^{N} \epsilon_{(n)j_1}^{(k)}(t)\cdots \epsilon_{(n)j_m}^{(k)}(t)|u_n^{(k)}(t)\rangle \\ &- 2\,\mathrm{Re}\langle \xi_n^{(k)}(t)|\sum_{m=1}^{N} \frac{\beta_m}{{}_N C_m} \sum_{j_1<\cdots<j_m}^{N} \epsilon_{(n-1)j_1}^{(k)}(t)\cdots \epsilon_{(n-1)j_m}^{(k)}(t)|u_{n-1}^{(k)}(t)\rangle.\end{aligned} \tag{A7}$$

From the definition of the notation $\{\bar{\epsilon}^{(k)}_{(n)j}(t)\}$ and $\{\epsilon^{(k)}_{(n)j}(t)\}$ in Eqs. (32) and (33), we note that

$$\epsilon^{(k)}_{(n)j}(t) = \bar{\epsilon}^{(k)}_{(n)j}(t) = \epsilon^{(k)}_{(n-1)j}(t) \quad (j \neq n) \tag{A8}$$

and

$$\epsilon^{(k)}_{(n)n}(t) = E^{(k)}_n(t), \quad \bar{\epsilon}^{(k)}_{(n)n}(t) = \bar{E}^{(k)}_n(t),$$
$$\epsilon^{(k)}_{(n-1)n}(t) = E^{(k-1)}_n(t). \tag{A9}$$

We divide the summation with respect to $\{j_1, \ldots, j_m\}$ into two parts, one of which does not involve n and the other involves n:

$$\sum_{j_1<\cdots<j_m}^{N} = \sum_{j_1<\cdots<j_m}^{N}{}^{(n)} + \sum_{j_1<\cdots<j_m}^{N} (\delta_{n,j_1} + \cdots + \delta_{n,j_m}). \tag{A10}$$

The Kronecker delta in Eq. (A10) originates from the fact that only one of the dummy indexes is equal to n because $j_1 < \cdots < j_m$. In Eq. (A7), the terms involved in the summation $\Sigma^N_{j_1<\cdots<j_m}(n)$ are canceled. The summation associated with $\Sigma^N_{j_1<\cdots<j_m}(\delta_{n,j_1}+\cdots+\delta_{n,j_m})$ is, for example, rewritten as

$$\begin{aligned}
&\sum_{m=1}^{N} \frac{\beta_m}{{}_N C_m} \sum_{j_1<\cdots<j_m}^{N} (\delta_{n,j_1} + \cdots + \delta_{n,j_m}) \bar{\epsilon}^{(k)}_{(n)j_1}(t) \cdots \bar{\epsilon}^{(k)}_{(n)j_m}(t) \\
&= \frac{\beta_1}{{}_N C_1} \bar{E}^{(k)}_n(t) + \frac{\beta_2}{{}_N C_2} \left[\sum_{n<j_2}^{N} \bar{E}^{(k)}_n(t) \bar{\epsilon}^{(k)}_{(n)j_2}(t) + \sum_{j_1<n}^{N} \bar{\epsilon}^{(k)}_{(n)j_1}(t) \bar{E}^{(k)}_n(t) \right] + \frac{\beta_3}{{}_N C_3} \left[\sum_{n<j_2<j_3}^{N} \bar{E}^{(k)}_n(t) \bar{\epsilon}^{(k)}_{(n)j_2}(t) \bar{\epsilon}^{(k)}_{(n)j_3}(t) \right. \\
&\quad \left. + \sum_{j_1<n<j_3}^{N} \bar{\epsilon}^{(k)}_{(n)j_1}(t) \bar{E}^{(k)}_n(t) \bar{\epsilon}^{(k)}_{(n)j_3}(t) + \sum_{j_1<j_2<n}^{N} \bar{\epsilon}^{(k)}_{(n)j_1}(t) \bar{\epsilon}^{(k)}_{(n)j_2}(t) \bar{E}^{(k)}_n(t) \right] + \cdots \\
&= \left\{ \beta_1 + \frac{N\beta_2}{{}_N C_2} \sum_{j_1}^{N}{}^{(n)} \epsilon^{(k)}_{(n)j_1}(t) + \frac{N\beta_3}{{}_N C_3} \sum_{j_1<j_2}^{N}{}^{(n)} \epsilon^{(k)}_{(n)j_1}(t) \epsilon^{(k)}_{(n)j_2}(t) + \cdots \right\} \frac{\bar{E}^{(k)}_n(t)}{N} \\
&= B_n{}^{(k)} \frac{\bar{E}^{(k)}_n(t)}{N},
\end{aligned} \tag{A11}$$

where $B_n{}^{(k)}$ is defined in Eq. (36). The substitution of Eq. (A11), etc., into Eq. (A7) yields

$$\begin{aligned}
\frac{d}{dt} P^{(k)}_n(t) + 2\,\mathrm{Re}\langle Y(t)|\delta u^{(k)}_n(t)\rangle &= [E^{(k)}_n(t) - \bar{E}^{(k)}_n(t)] \frac{2}{N} \mathrm{Re}\langle \xi^{(k)}_n(t)|B_n|u^{(k)}_n(t)\rangle + [\bar{E}^{(k)}_n(t) - \bar{E}^{(k-1)}_n(t)] \frac{2}{N} \mathrm{Re}\langle \xi^{(k)}_n(t)|B_n|u^{(k)}_{n-1}(t)\rangle \\
&= \frac{2}{N\lambda(t)} \{ [E^{(k)}_n(t) - \bar{E}^{(k)}_n(t)] E^{(k)}_n(t) + [\bar{E}^{(k)}_n(t) - E^{(k-1)}_n(t)] \bar{E}^{(k)}_n(t) \}.
\end{aligned} \tag{A12}$$

If we integrate Eq. (A12) over $t \in [0, t_f]$, we have

$$\delta F_n = \int_0^{t_f} \frac{dt}{N\lambda(t)} \{ [E^{(k)}_n(t)]^2 + [E^{(k)}_n(t) - \bar{E}^{(k)}_n(t)]^2 + [\bar{E}^{(k)}_n(t) - E^{(k-1)}_n(t)]^2 - [E^{(k-1)}_n(t)]^2 \}. \tag{A13}$$

Equation (A13) is used to rewrite Eq. (A4) in terms of controls. If we substitute the resulting expression into Eqs. (A1) and (A2), we have

$$\delta J_I^{(k,k-1)} = \sum_{n=1}^{N} \delta F_n - \delta G^{(k,k-1)} = \int_0^{t_f} \frac{dt}{N\lambda(t)} \sum_{n=1}^{N} \{ [E^{(k)}_n(t) - \bar{E}^{(k)}_n(t)]^2 + [\bar{E}^{(k)}_n(t) - E^{(k-1)}_n(t)]^2 \} \geq 0, \tag{A14}$$

which proves the monotonic convergence behavior of the algorithm.

[1] D. J. Tannor, *Introduction to Quantum Mechanics* (University Science Books, Sausalito, CA, 2007), Chap. 16.
[2] A. P. Peirce, M. A. Dahleh, and H. Rabitz, Phys. Rev. A **37**, 4950 (1988).
[3] R. Kosloff, S. A. Rice, P. Gaspard, S. Tersigni, and D. J. Tannor, Chem. Phys. **139**, 201 (1989).
[4] W. Zhu, J. Botina, and H. Rabitz, J. Chem. Phys. **108**, 1953 (1998).
[5] Y. Ohtsuki, W. Zhu, and H. Rabitz, J. Chem. Phys. **110**, 9825 (1999).
[6] Y. Ohtsuki and H. Rabitz, CRM Proc. Lect. Notes **33**, 163 (2003).
[7] Y. Maday and G. Turinici, J. Chem. Phys. **118**, 8191 (2003).
[8] Y. Ohtsuki, J. Chem. Phys. **119**, 661 (2003).
[9] Y. Ohtsuki, G. Turinici, and H. Rabitz, J. Chem. Phys. **120**, 5509 (2004).
[10] Y. Ohtsuki, Y. Teranishi, P. Saalfrank, G. Turinici, and H. Rabitz, Phys. Rev. A **75**, 033407 (2007).
[11] J. Somlói, V. A. Kazakov, and D. J. Tannor, Chem. Phys. **172**, 85 (1993).
[12] A. Bartana, R. Kosloff, and D. J. Tannor, J. Chem. Phys. **106**, 1435 (1997).
[13] P. B. Corkum, M. Yu Ivanov, and J. S. Wright, Annu. Rev. Phys. Chem. **48**, 387 (1997).
[14] H. Stapelfeldt and T. Seideman, Rev. Mod. Phys. **75**, 543 (2003) and references therein.
[15] F. Rosca-Pruna and M. J. J. Vrakking, Phys. Rev. Lett. **87**, 153902 (2001).
[16] I. V. Litvinyuk, K. F. Lee, P. W. Dooley, D. M. Rayner, D. M. Villeneuve, and P. B. Corkum, Phys. Rev. Lett. **90**, 233003 (2003).
[17] T. Suzuki, S. Minemoto, T. Kanai, and H. Sakai, Phys. Rev. Lett. **92**, 133005 (2004).
[18] H. Ohmura, N. Saito, and M. Tachiya, Phys. Rev. Lett. **96**, 173001 (2006).
[19] H. Hasegawa and Y. Ohshima, Phys. Rev. A **74**, 061401(R) (2006).
[20] R. J. Levis, G. M. Menkir, and H. Rabitz, Science **292**, 709 (2001).
[21] B. J. Sussman, D. Townsend, M. Yu Ivanov, and A. Stolow, Science **314**, 278 (2006).
[22] G. G. Balint-Kurti, F. R. Manby, Q. Ren, M. Artamonov, T.-S. Ho, and H. Rabitz, J. Chem. Phys. **122**, 084110 (2005).
[23] Q. Ren, G. G. Balint-Kurti, F. R. Manby, M. Artamonov, T.-S. Ho, and H. Rabitz, J. Chem. Phys. **124**, 014111 (2006).
[24] S. Zou, G. G. Balint-Kurti, and F. R. Manby, J. Chem. Phys. **127**, 044107 (2007).
[25] R. S. Judson and H. Rabitz, Phys. Rev. Lett. **68**, 1500 (1992).
[26] D. Sugny, C. Kontz, and H. R. Jauslin, Phys. Rev. A **74**, 053411 (2006).
[27] E. Hertz, A. Rouzée, S. Guérin, B. Lavorel, and O. Faucher, Phys. Rev. A **75**, 031403(R) (2007).
[28] J. Salomon, C. M. Dion, and G. Turinici, J. Chem. Phys. **123**, 144310 (2005).
[29] A. Ben Haj-Yedder, A. Auger, C. M. Dion, E. Cancés, A. Keller, C. Le Bris, and O. Atabek, Phys. Rev. A **66**, 063401 (2002).
[30] Y. Ohtsuki, K. Nakagami, Y. Fujimura, W. Zhu, and H. Rabitz, J. Chem. Phys. **114**, 8867 (2001).
[31] K. Nakagami, Y. Mizumoto, and Y. Ohtsuki, (unpublished).
[32] B. Friedrich and D. Herschbach, Phys. Rev. Lett. **74**, 4623 (1995).
[33] T. Seideman and E. Hamilton, Adv. At., Mol., Opt. Phys. **52**, 289 (2005).